Letter

Magic angles in equal-twist trilayer graphene

Fedor K. Popov and Grigory Tarnopolsky

Department of Physics, New York University, New York, New York 10003, USA
and Department of Physics, Carnegie Mellon University, Pittsburgh, Pennsylvania 15213, USA

We consider a configuration of three stacked graphene monolayers with equal consecutive twist angles θ. Remarkably, in the chiral limit when interlayer coupling terms between AA sites of the moiré pattern are neglected we find four perfectly flat bands (per valley and spin) at a sequence of magic angles which are exactly equal to the twisted bilayer graphene (TBG) magic angles divided by $\sqrt{2}$. Therefore, the first magic angle for equal-twist trilayer graphene (eTTG) in the chiral limit is $\theta_* \approx 1.05°/\sqrt{2} \approx 0.74°$. We prove this relation analytically and show that the Bloch states of the eTTG's flat bands are nonlinearly related to those of TBG. Additionally, we show that at the magic angles, the upper and lower bands must touch the four exactly flat bands at the Dirac point of the middle graphene layer. Finally, we explore the eTTG's spectrum away from the chiral limit through numerical analysis.

DOI: 10.1103/PhysRevB.108.L081124

I. INTRODUCTION

The remarkable theoretical predictions [1,2] of the fascinating properties of twisted bilayer graphene (TBG) at a special ("magic") angle $\theta_* \approx 1.05°$ and experimental realization of this configuration have uncovered an array of correlated phenomena, such as Mott-insulating and superconducting phases [3–5]. This tantalizing discovery has sparked an avalanche of further experimental and theoretical research [6–32], aimed at gaining a deeper understanding of the underlying physics of these van der Waals heterostructures.

The investigation of multiple graphene layer configurations, such as twisted trilayer graphene, is a natural generalization of the study of twisted bilayer graphene [33–40]. The multilayer systems possess a greater number of parameters, which enhance their tunability. The initial theoretical investigation of twisted trilayer graphene (TTG) [33,34] unveiled a similar flattening of electronic bands at various "magic" angles, which ultimately led to experimental discovery of correlated phenomena and other intriguing physics [41–46]. The interacting effects in such systems are under persistent theoretical investigation [47–49]. Other twisted graphene multilayer systems were discussed theoretically [50–55] and realized experimentally [56–58] where similar interacting effects were discovered.

In this Letter, we focus on twisted trilayer graphene with equal small consecutive twist angles θ. We refer to such a system as equal-twist trilayer graphene (eTTG), and it is schematically represented in Fig 1. This particular twist configuration of TTG has already been discussed in [34,37–40].

The main result of this Letter is exact relations between magic angles and perfectly flat band wave functions of eTTG and TBG systems in the chiral limit (i.e., the limit when interlayer hopping terms between AA sites of the moiré pattern are neglected). We show below that the magic angles of these systems are related as

$$\theta_{\text{eTTG}} = \theta_{\text{TBG}}/\sqrt{2}. \tag{1}$$

Therefore the first magic angle of eTTG is $\theta_* \approx 1.05°/\sqrt{2} \approx 0.74°$. Remarkably this relation is exactly inverse of the relation found in [33] for alternating-twist trilayer graphene (aTTG):

$$\theta_{\text{aTTG}} = \theta_{\text{TBG}}\sqrt{2}. \tag{2}$$

In contrast to the aTTG case the relation (1) can be established only in the chiral limit. Moreover the relation between the Bloch states of the eTTG's exactly flat bands and those of TBG is valid only at the magic angles.

The Letter is organized as follows. In Sec. II we formulate the continuum model for twisted trilayer graphene and then consider the case of the equal-twist configuration of trilayer graphene (eTTG). We obtain the Hamiltonian for such a configuration in the chiral limit. In Sec. III we present our main result, namely the relation between magic angels and perfectly flat band Bloch states of eTTG and TBG in the chiral limit. In Sec. IV we discuss theoretical and experimental challenges arising from investigation of eTTG away from the chiral limit.

II. CONTINUUM MODEL FOR TWISTED TRILAYER GRAPHENE

We consider a system of three stacked graphene monolayers, where each layer $\ell = 1, 2, 3$ is rotated counterclockwise by an angle θ_ℓ around an atom site and then shifted by a vector $\mathbf{d}_\ell$, so atoms in each layer are parametrized by $\mathbf{r} = R_{\theta_\ell}(\mathbf{R} + \tau_\alpha) + \mathbf{d}_\ell$, where $R_\theta = e^{-i\theta\sigma_y}$ is the rotation matrix and $\mathbf{R}$ and τ_α run over the lattice and sublattice sites. The continuum model Hamiltonian for twisted trilayer graphene can be written as [33]

$$H = \begin{pmatrix} -iv_F \boldsymbol{\sigma}_{\theta_1}\nabla & T^{12}(\mathbf{r}-\mathbf{d}_{12}) & 0 \\ T^{12\dagger}(\mathbf{r}-\mathbf{d}_{12}) & -iv_F \boldsymbol{\sigma}_{\theta_2}\nabla & T^{23}(\mathbf{r}-\mathbf{d}_{23}) \\ 0 & T^{23\dagger}(\mathbf{r}-\mathbf{d}_{23}) & -iv_F \boldsymbol{\sigma}_{\theta_3}\nabla \end{pmatrix},$$

where $v_F \approx 10^6$ m/s is the monolayer graphene Fermi velocity, $\boldsymbol{\sigma}_\theta \equiv e^{i\frac{\theta}{2}\sigma_z}\boldsymbol{\sigma}e^{-i\frac{\theta}{2}\sigma_z}$, $\boldsymbol{\sigma} = (\sigma_x, \sigma_y)$, and $\mathbf{d}_{\ell\ell'} = \frac{1}{2}[\mathbf{d}_\ell + \mathbf{d}_{\ell'} +$
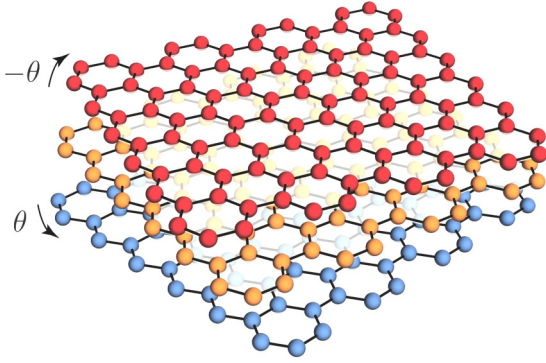
FIG. 1. A schematic illustration of the equal-twist trilayer graphene: the top and bottom layers are twisted by an angle θ in opposite directions relative to the middle layer.

FIG. 2. (a) Original Brillouin zones of three graphene layers with their Dirac points K_1, K_2, and K_3. Three layers are consecutively twisted by the same angle θ, so $|\mathbf{q}_1^{12}| = |\mathbf{q}_1^{23}|$. (b) Moiré Brillouin zone for eTTG. We neglect a relative rotation between vectors $\mathbf{q}_1^{12}$ and $\mathbf{q}_1^{23}$ and denote them by $\mathbf{q}_1$. The wave vector $\mathbf{k}$ is zero at the Dirac point K_2.

$i \cot(\theta_{\ell'\ell}/2)\sigma_y(\mathbf{d}_\ell - \mathbf{d}_{\ell'})]$ is the moiré pattern displacement vector. The moiré potential between adjacent layers ℓ and ℓ' is

$$T^{\ell\ell'}(\mathbf{r}) = \sum_{n=1}^{3} T_n^{\ell\ell'} e^{-i\mathbf{q}_n^{\ell\ell'}\mathbf{r}}, \qquad (3)$$

where $T_{n+1}^{\ell\ell'} = w_{AA}^{\ell\ell'}\sigma_0 + w_{AB}^{\ell\ell'}(\sigma_x \cos n\phi + \sigma_y \sin n\phi)$ and

$$\mathbf{q}_1^{\ell\ell'} = 2k_D \sin(\theta_{\ell'\ell}/2)R_{\phi_{\ell\ell'}}(0,-1), \quad \mathbf{q}_{2,3}^{\ell\ell'} = R_{\pm\phi}\mathbf{q}_1^{\ell\ell'}, \qquad (4)$$

with $\theta_{\ell\ell'} = \theta_\ell - \theta_{\ell'}$, $\phi_{\ell\ell'} = (\theta_\ell + \theta_{\ell'})/2$, $\phi = 2\pi/3$, and $k_D = 4\pi/3\sqrt{3}a$ is the Dirac momentum of the monolayer graphene with lattice constant $a = 1.42$ Å. The coupling between adjacent layers ℓ and ℓ' is characterized by two parameters $w_{AA}^{\ell\ell'}$ and $w_{AB}^{\ell\ell'}$ representing intra- and inter-sublattice couplings. The chiral limit corresponds to $w_{AA}^{\ell\ell'} = 0$.

In this Letter we consider only a trilayer configuration with two equal consecutive twist angles θ; thus we take $\theta_1 = -\theta$, $\theta_2 = 0$, and $\theta_3 = \theta$ (magic angles in the chiral limit of a general TTG configuration with $\theta_{12}/\theta_{23} = p/q$, where p and q are coprime integers and are discussed elsewhere [59]; see also [34]). Moreover we assume that there is no displacement between layers $\mathbf{d}_{\ell\ell'} = 0$ (for the aTTG case it was shown in [60] that this is energetically favorable stacking configuration). Finally for a small angle θ we set $\phi_{\ell\ell'} = 0$ leading to $\mathbf{q}_1^{12} = \mathbf{q}_1^{23} = \mathbf{q}_1$ [34]. Thus we obtain the following Hamiltonian for eTTG:

$$H_{\text{eTTG}} = \begin{pmatrix} -iv_F\boldsymbol{\sigma}_{-\theta}\boldsymbol{\nabla} & T(\mathbf{r}) & 0 \\ T^\dagger(\mathbf{r}) & -iv_F\boldsymbol{\sigma}\boldsymbol{\nabla} & T(\mathbf{r}) \\ 0 & T^\dagger(\mathbf{r}) & -iv_F\boldsymbol{\sigma}_\theta\boldsymbol{\nabla} \end{pmatrix}, \qquad (5)$$

where we also assumed that the coupling parameters w_{AA} and w_{AB} do not depend on layers. The moiré Brillouin zone (mBZ) for this Hamiltonian is depicted in Fig. 2. The reciprocal moiré lattice is generated by vectors $\mathbf{b}_{1,2} = \mathbf{q}_{2,3} - \mathbf{q}_1$. In the coordinate space the eTTG configuration forms a single moiré lattice that is spanned by the lattice vectors $\mathbf{a}_{1,2} = (4\pi/3k_\theta)(\pm\sqrt{3}/2, 1/2)$, with $k_\theta = 2k_D \sin(\theta/2)$, and we neglect the effects of the moiré lattice [37]. It is useful to introduce complex coordinates $z, \bar{z} = \mathbf{r}_x \pm i\mathbf{r}_y$ in real space and $k, \bar{k} = \mathbf{k}_1 \pm i\mathbf{k}_2$ in momentum space. The Hamiltonian
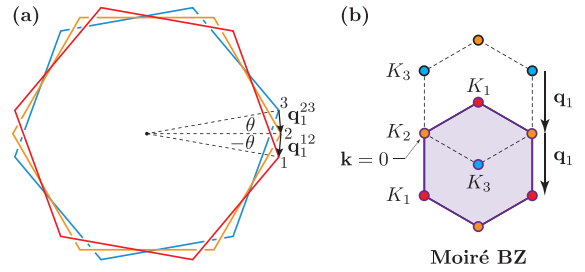
(5) acts on a spinor $\Phi(\mathbf{r}) = (\phi_1, \eta_1, \phi_2, \eta_2, \phi_3, \eta_3)$, where the indices 1,2,3 represent the graphene layer.

For a small twist angle θ we can neglect the phase factors in the Pauli matrices $\boldsymbol{\sigma}_{\pm\theta} \to \boldsymbol{\sigma}$. Introducing the dimensionless variable $\alpha = w_{AB}/(v_F k_\theta)$, and writing the Hamiltonian (5) in the sublattice basis $\Phi(\mathbf{r}) = (\phi_1, \phi_2, \phi_3, \eta_1, \eta_2, \eta_3)$, we obtain

$$\mathcal{H}_{\text{eTTG}} = \begin{pmatrix} \mathcal{M}(\mathbf{r}) & \mathcal{D}_3^\dagger(\mathbf{r}) \\ \mathcal{D}_3(\mathbf{r}) & \mathcal{M}(\mathbf{r}) \end{pmatrix}, \qquad (6)$$

where we have rescaled coordinates $\mathbf{r} \to k_\theta \mathbf{r}$ and the Hamiltonian, so the energies of (6) are measured in units of $v_F k_\theta$. The operators $\mathcal{D}_3$ and $\mathcal{M}$ are

$$\mathcal{D}_3(\mathbf{r}) = \begin{pmatrix} -2i\bar{\partial} & \alpha U(\mathbf{r}) & 0 \\ \alpha U(-\mathbf{r}) & -2i\bar{\partial} & \alpha U(\mathbf{r}) \\ 0 & \alpha U(-\mathbf{r}) & -2i\bar{\partial} \end{pmatrix},$$

$$\mathcal{M}(\mathbf{r}) = \frac{w_{AA}}{w_{AB}} \begin{pmatrix} 0 & U_0(\mathbf{r}) & 0 \\ U_0(-\mathbf{r}) & 0 & U_0(\mathbf{r}) \\ 0 & U_0(-\mathbf{r}) & 0 \end{pmatrix}, \qquad (7)$$

where the potentials $U(\mathbf{r}) = \sum_{n=1}^{3} \omega^{n-1} e^{-i\mathbf{q}_n \mathbf{r}}$ and $U_0(\mathbf{r}) = \sum_{n=1}^{3} e^{-i\mathbf{q}_n \mathbf{r}}$, $\omega = e^{i\phi}$, $\mathbf{q}_n = R_{(n-1)\phi}(0,-1)$, and we introduced derivatives $\partial, \bar{\partial} = \frac{1}{2}(\partial_x \mp i\partial_y)$. The Bloch states $\Phi_\mathbf{k}(\mathbf{r}) = (\phi_\mathbf{k}(\mathbf{r}), \eta_\mathbf{k}(\mathbf{r}))$ of (6) are parametrized by the wave vector $\mathbf{k}$ from the mBZ and satisfy the following boundary conditions:

$$\Phi_\mathbf{k}(\mathbf{r} + \mathbf{a}_{1,2}) = e^{i\mathbf{k}\mathbf{a}_{1,2}} U_\phi^{(3)} \Phi_\mathbf{k}(\mathbf{r}), \qquad (8)$$

where the matrix $U_\phi^{(3)} = \mathbb{1}_{AB} \otimes \text{diag}(\omega, 1, \omega^*)$.

III. RELATION TO THE TWISTED BILAYER GRAPHENE

In this section we show that eTTG Hamiltonian (6) has an infinite series of magic angles and exactly flat bands in the chiral limit $w_{AA} = 0$. Moreover the magic angles and the Bloch states of the eTTG's flat bands are related to those of TBG. Namely, if TBG has two exactly flat bands at the magic angle θ_{TBG} then eTTG must have four exactly flat bands at the magic angle at $\theta_{\text{eTTG}} = \theta_{\text{TBG}}/\sqrt{2}$.

The Hamiltonian for TBG in the chiral limit has the following form in the sublattice basis [29]:

$$\mathcal{H}_{TBG} = \begin{pmatrix} 0 & \mathcal{D}^\dagger(\mathbf{r}) \\ \mathcal{D}(\mathbf{r}) & 0 \end{pmatrix}, \quad \mathcal{D}(\mathbf{r}) = \begin{pmatrix} -2i\bar{\partial} & \alpha U(\mathbf{r}) \\ \alpha U(-\mathbf{r}) & -2i\bar{\partial} \end{pmatrix}. \quad (9)$$

The Bloch's wave functions $\Psi_{\mathbf{k}}(\mathbf{r}) = (\psi_{\mathbf{k}}(\mathbf{r}), \chi_{\mathbf{k}}(\mathbf{r}))$ satisfy the boundary conditions

$$\Psi_{\mathbf{k}}(\mathbf{r} + \mathbf{a}_{1,2}) = e^{i\mathbf{k}\mathbf{a}_{1,2}} U_\phi^{(2)} \Psi_{\mathbf{k}}(\mathbf{r}), \quad (10)$$

where $U_\phi^{(2)} = \mathbb{1}_{AB} \otimes \text{diag}(1, \omega^*)$. This Hamiltonian has two exactly flat bands at zero energy over the entire mBZ:

$$\mathcal{H}_{TBG} \Psi_{\mathbf{k}}(\mathbf{r}) = \varepsilon_0(\mathbf{k}) \Psi_{\mathbf{k}}(\mathbf{r}), \quad \varepsilon_0(\mathbf{k}) = 0,$$

at the infinite series of magic angles $\alpha = 0.586, 2.221, \ldots$. These flat bands are formed by the Bloch states $\Psi_{\mathbf{k}} = (\psi_{\mathbf{k}}, 0)$ and $\hat{\Psi}_{\mathbf{k}} = (0, \chi_{\mathbf{k}})$, where the functions $\psi_{\mathbf{k}}$ satisfy the equation

$$\mathcal{D}(\mathbf{r}) \psi_{\mathbf{k}}(\mathbf{r}) = 0, \quad \psi_{\mathbf{k}}(\mathbf{r} + \mathbf{a}_{1,2}) = e^{i\mathbf{k}\mathbf{a}_{1,2}} U_\phi \psi_{\mathbf{k}}(\mathbf{r}), \quad (11)$$

with $U_\phi = \text{diag}(1, \omega^*)$ and the functions $\chi_{\mathbf{k}}$ satisfy $\mathcal{D}^\dagger \chi_{\mathbf{k}} = 0$ with the same boundary conditions.

Let us assume we have two wave functions $\psi_{\mathbf{k}}$ and $\psi_{\mathbf{k}'}$ at wave vectors $\mathbf{k}$ and $\mathbf{k}'$ of the mBZ [we notice that the eTTG and TBG Hamiltonians (6) and (9) have identical mBZ]. These wave functions are two-component spinors: $\psi_{\mathbf{k}} = (\psi_{\mathbf{k}1}, \psi_{\mathbf{k}2})$ and $\psi_{\mathbf{k}'} = (\psi_{\mathbf{k}'1}, \psi_{\mathbf{k}'2})$ and we can construct the following three-component wave function using their components:

$$\phi_{\mathbf{k}+\mathbf{k}'+\mathbf{q}_1}(\mathbf{r}) = \psi_{\mathbf{k}}(\mathbf{r}) \times \psi_{\mathbf{k}'}(\mathbf{r})$$
$$\equiv \begin{pmatrix} \psi_{\mathbf{k}1}(\mathbf{r}) \psi_{\mathbf{k}'1}(\mathbf{r}) \\ \frac{1}{\sqrt{2}} [\psi_{\mathbf{k}1}(\mathbf{r}) \psi_{\mathbf{k}'2}(\mathbf{r}) + \psi_{\mathbf{k}2}(\mathbf{r}) \psi_{\mathbf{k}'1}(\mathbf{r})] \\ \psi_{\mathbf{k}2}(\mathbf{r}) \psi_{\mathbf{k}'2}(\mathbf{r}) \end{pmatrix}, \quad (12)$$

where the subscript of the functions indicates the location at the BZ. Thus one can check that the resulted function ϕ satisfy (8) for the point $\mathbf{k} + \mathbf{k}' + \mathbf{q}_1$ of BZ. This construction allows, in principle, to find several wave functions at the given point of BZ, but we will show that they are linearly dependent. It is possible to check that this wave function satisfies the zero-energy equation of eTTG,

$$\mathcal{D}_3(\mathbf{r}) \phi_{\mathbf{k}+\mathbf{k}'+\mathbf{q}_1} = 0, \quad (13)$$

and the boundary conditions (8), provided we use the following relation between the parameters α (twist angles) of eTTG and TBG:

$$\alpha_{eTTG} = \sqrt{2} \alpha_{TBG} \quad (\theta_{eTTG} = \theta_{TBG}/\sqrt{2}). \quad (14)$$

Hence we constructed zero-energy Bloch states $\Phi_{\mathbf{k}+\mathbf{k}'+\mathbf{q}_1} = (\phi_{\mathbf{k}+\mathbf{k}'+\mathbf{q}_1}, 0)$ of the Hamiltonian $\mathcal{H}_{eTTG}$ in the chiral limit $w_{AA} = 0$. Similarly we can construct zero-energy Bloch states $\hat{\Phi}_{\mathbf{k}+\mathbf{k}'+\mathbf{q}_1} = (0, \eta_{\mathbf{k}+\mathbf{k}'+\mathbf{q}_1})$ using the functions $\chi_{\mathbf{k}}$ and $\chi_{\mathbf{k}'}$ of TBG. The spectrum of eTTG in the chiral limit at the first two magic angles is depicted in Fig. 3 and we listed the first four magic angles in TBG and eTTG in Table I. Below we write explicit expressions for the eTTG flat bands Bloch states and explain why there are four exactly flat bands in this case.
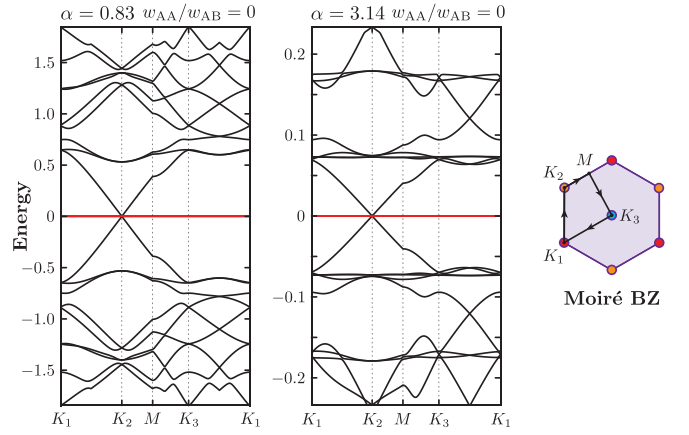

FIG. 3. Spectrum of the equal-twist trilayer graphene Hamiltonian (6) in the chiral limit ($w_{AA}/w_{AB} = 0$) at the first two magic angles $\alpha = 0.83$ and $\alpha = 3.14$. There are four exactly flat bands at zero energy (highlighted in red).

It was derived in [29] that the wave functions $\psi_{\mathbf{k}}(\mathbf{r})$ in (11) have the form

$$\psi_{\mathbf{k}}(\mathbf{r}) = f_{\mathbf{k}}(z) \psi_K(\mathbf{r}),$$
$$f_{\mathbf{k}}(z) = e^{i\frac{\mathbf{k}\mathbf{a}_1}{a_1}z} \frac{\vartheta_1([z - (1-ik)z_0]/a_1|\omega)}{\vartheta_1((z - z_0)/a_1|\omega)}, \quad (15)$$

where $a_{1,2} = (\mathbf{a}_{1,2})_x + i(\mathbf{a}_{1,2})_y$, $z_0 = \frac{1}{3}(a_1 - a_2)$, and $\psi_K = (\psi_{K,1}, \psi_{K,2})$ is a solution of (11) at the Dirac point K, which corresponds to $\mathbf{k} = 0$ (this solution exists for an arbitrary twist angle). The theta function $\vartheta_1(z|\tau)$ is defined as

$$\vartheta_1(z|\tau) = \sum_{n=-\infty}^{+\infty} e^{i\pi\tau(n+\frac{1}{2})^2} e^{2\pi i(z-\frac{1}{2})(n+\frac{1}{2})}, \quad (16)$$

and has zeros at $z = m + n\tau$. At the magic angles, the function $\psi_K(\mathbf{r})$ has a zero at the point $\mathbf{r}_0 = \frac{1}{3}(\mathbf{a}_1 - \mathbf{a}_2)$. This zero cancels with the zero of the theta function in (15), making $\psi_{\mathbf{k}}(\mathbf{r})$ finite. The function $\psi_{\mathbf{k}}(\mathbf{r})$ has zero at $z = (1-ik)z_0$ due to the theta function in the numerator.

Using these results for TBG we obtain for the eTTG zero-energy wave functions

$$\phi_{\mathbf{k}}(\mathbf{r}) = f_{\mathbf{k}'}(z) f_{\mathbf{k}-\mathbf{k}'-\mathbf{q}_1}(z) \phi_{K_1}(\mathbf{r}), \quad (17)$$

where $\phi_{K_1} = ((\psi_{K,1})^2, \sqrt{2}\psi_{K,1}\psi_{K,2}, (\psi_{K,2})^2)$ is the zero-energy solution at the Dirac point K_1 of eTTG (corresponds to $\mathbf{k} = \mathbf{q}_1$). The functions (17) have two zeros (or a double zero) in the moiré lattice unit cell and thus there are only two linearly independent solutions (17) at each point of the mBZ [61] and using Eq. (12) for different wave functions of TBG we would always get a linear combination of these basis

TABLE I. Comparison between magic angles for TBG and eTTG in the chiral limit ($w_{AA}/w_{AB} = 0$).

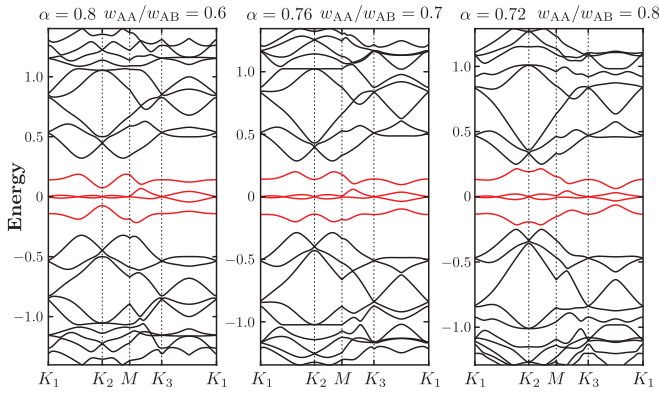|	α_1	α_2	α_3	α_4
TBG	0.586	2.221	3.75	5.276
eTTG	0.829	3.141	5.30	7.461

FIG. 4. Spectrum of the equal-twist trilayer graphene Hamiltonian (6) for $w_{AA}/w_{AB} = 0.6, 0.7, 0.8$ at the twist angles $\alpha = 0.8, 0.76, 0.72$ close to the first magic angle $\alpha = 0.83$. For each ratio w_{AA}/w_{AB} we chose a twist angle such that it minimizes the bandwidth of the first two lowest energy bands. The four lowest energy bands are highlighted in red. These bands are exactly flat in the chiral limit ($w_{AA}/w_{AB} = 0$) at the magic angle.

solutions. There is a freedom to choose a basis of two linearly independent solutions $\phi_{\mathbf{k}}^{(1)}$ and $\phi_{\mathbf{k}}^{(2)}$ and one possible choice is

$$\phi_{\mathbf{k}}^{(1)}(\mathbf{r}) = f_{\mathbf{k}}(z)f_{-\mathbf{q}_1}(z)\phi_{K_1}(\mathbf{r}),$$
$$\phi_{\mathbf{k}}^{(2)}(\mathbf{r}) = f_{\mathbf{k}+\mathbf{q}_1}(z)f_{-2\mathbf{q}_1}(z)\phi_{K_1}(\mathbf{r}). \quad (18)$$

We notice that these functions are not necessarily orthogonal. It is possible to construct an orthogonal set following [61]. Hence the functions $\Phi_{\mathbf{k}} = (\phi_{\mathbf{k}}, 0)$ and $\hat{\Phi}_{\mathbf{k}} = (0, \eta_{\mathbf{k}})$ comprise four exactly flat bands.

Now we show that at the magic angles of the chiral eTTG the upper and lower bands touch the four exactly flat bands at the Dirac point K_2, as can be seen in Fig. 3. The emergence of two additional zero modes $\tilde{\Phi}_{K_2} = (\tilde{\phi}_{K_2}, 0)$ and $\tilde{\Phi}_{K_2} = (0, \tilde{\eta}_{K_2})$ at the magic angles is related to existence of unphysical singular solutions $\tilde{\psi}_{\mathbf{k}}(\mathbf{r})$ and $\tilde{\chi}_{\mathbf{k}}(\mathbf{r})$ of the chiral TBG Hamiltonian at the magic angles [62]. As was shown in [62] Eq. (11), apart from the regular solution $\psi_{\mathbf{k}}(\mathbf{r})$ in (15), admits a singular solution $\tilde{\psi}_{\mathbf{k}}(\mathbf{r})$ which has a pole instead of a zero. Since this solution is singular it never appears in the spectrum of TBG. But in the case of eTTG the relation (12) allows one to construct a nonsingular wave function $\tilde{\phi}_{K_2}(\mathbf{r})$ by multiplying components of the function $\tilde{\psi}_{\mathbf{k}}$ with the pole by the components of the function $\psi_{\mathbf{k}'}$ with zero, such that the pole and zero are at the same point of the moiré unit cell and cancel each other. This is possible provided $\mathbf{k} + \mathbf{k}' + \mathbf{q}_1 = 0$.

In spite of infinitely many combinations $\mathbf{k}$ and $\mathbf{k}'$ satisfying this constraint, there is only a single linearly independent wave function $\tilde{\phi}_{K_2}(\mathbf{r})$ and for concreteness we choose $\mathbf{k} = 0$ and $\mathbf{k}' = -\mathbf{q}_1$, so we can write

$$\tilde{\phi}_{K_2}(\mathbf{r}) = \tilde{\psi}_K(\mathbf{r}) \times \psi_{K'}(\mathbf{r}), \quad (19)$$

where $\tilde{\psi}_K$ and $\psi_{K'}$ are the singular and regular solutions of Eq. (11) at the TBG Dirac points K ($\mathbf{k} = 0$) and K' ($\mathbf{k} = -\mathbf{q}_1$), respectively. A similar construction applies to the function $\tilde{\eta}_{K_2}(\mathbf{r})$.

Finally in Fig. 4 we plot a spectrum of the eTTG Hamiltonian (6) away from the chiral limit. We see that the four lowest energy bands are sensitive to the coupling parameter w_{AA}. Nevertheless the first two lowest energy bands remain relatively flat in a small range of twist angles close to the first eTTG magic angle $\alpha = 0.83$.

IV. DISCUSSION

In conclusion, we related magic angles and the Bloch states of the exactly flat bands of eTTG to those of TBG in the chiral limit. The electronic band structure of TBG has been extensively studied [29,62–67]. We remark that the relation between the alternating-twist trilayer graphene (aTTG) and TBG found in [33] is a linear algebraic relation between the aTTG and TBG Hamiltonians and works for any twist angles α and ratio of the coupling parameters w_{AA}/w_{AB}. In contrast, the relation between the eTTG and TBG zero-energy Bloch states is nonlinear and is valid only at the magic angles or Dirac points. In general the rest of the spectrum of eTTG and TBG at the magic angles is different.

Finally we remark that the current experimental works did not investigate eTTG at the range of angles close to the first magic angle $\theta_* \approx 0.74°$ predicted in this Letter. Although the lowest energy bands of eTTG near the magic angle lose their perfect flatness away from the chiral limit, it is still possible that these bands "remember" the holomorphic structure of the Bloch states (18) in the chiral limit, similarly to the case of TBG [68], and this could potentially pave the way for exciting new discoveries.

[1] R. Bistritzer and A. H. MacDonald, Moiré bands in twisted double-layer graphene, Proc. Natl. Acad. Sci. USA **108**, 12233 (2011).

[2] E. Suárez Morell, J. D. Correa, P. Vargas, M. Pacheco, and Z. Barticevic, Flat bands in slightly twisted bilayer graphene: Tight-binding calculations, Phys. Rev. B **82**, 121407(R) (2010).

[3] Y. Cao, V. Fatemi, S. Fang, K. Watanabe, T. Taniguchi, E. Kaxiras, and P. Jarillo-Herrero, Unconventional superconductivity in magic-angle graphene superlattices, Nature (London) **556**, 43 (2018).

[4] Y. Cao, V. Fatemi, A. Demir, S. Fang, S. L. Tomarken, J. Y. Luo, J. D. Sanchez-Yamagishi, K. Watanabe, T. Taniguchi, E. Kaxiras, R. C. Ashoori, and P. Jarillo-Herrero, Correlated

insulator behaviour at half-filling in magic-angle graphene superlattices, Nature (London) **556**, 80 (2018).

[5] M. Yankowitz, S. Chen, H. Polshyn, Y. Zhang, K. Watanabe, T. Taniguchi, D. Graf, A. F. Young, and C. R. Dean, Tuning superconductivity in twisted bilayer graphene, Science **363**, 1059 (2019).

[6] H. C. Po, L. Zou, A. Vishwanath, and T. Senthil, Origin of Mott Insulating Behavior and Superconductivity in Twisted Bilayer Graphene, Phys. Rev. X **8**, 031089 (2018).

[7] A. Thomson, S. Chatterjee, S. Sachdev, and M. S. Scheurer, Triangular antiferromagnetism on the honeycomb lattice of twisted bilayer graphene, Phys. Rev. B **98**, 075109 (2018).

[8] L. Zou, H. C. Po, A. Vishwanath, and T. Senthil, Band structure of twisted bilayer graphene: Emergent symmetries, commensurate approximants, and Wannier obstructions, Phys. Rev. B **98**, 085435 (2018).

[9] F. Guinea and N. R. Walet, Electrostatic effects, band distortions, and superconductivity in twisted graphene bilayers, Proc. Natl. Acad. Sci. USA **115**, 13174 (2018).

[10] S. Carr, S. Fang, P. Jarillo-Herrero, and E. Kaxiras, Pressure dependence of the magic twist angle in graphene superlattices, Phys. Rev. B **98**, 085144 (2018).

[11] Y. Su and S.-Z. Lin, Pairing symmetry and spontaneous vortex-antivortex lattice in superconducting twisted-bilayer graphene: Bogoliubov–de Gennes approach, Phys. Rev. B **98**, 195101 (2018).

[12] J. González and T. Stauber, Kohn-Luttinger Superconductivity in Twisted Bilayer Graphene, Phys. Rev. Lett. **122**, 026801 (2019).

[13] F. Wu, T. Lovorn, E. Tutuc, I. Martin, and A. H. MacDonald, Topological Insulators in Twisted Transition Metal Dichalcogenide Homobilayers, Phys. Rev. Lett. **122**, 086402 (2019).

[14] D. K. Efimkin and A. H. MacDonald, Helical network model for twisted bilayer graphene, Phys. Rev. B **98**, 035404 (2018).

[15] N. F. Q. Yuan and L. Fu, Model for the metal-insulator transition in graphene superlattices and beyond, Phys. Rev. B **98**, 045103 (2018).

[16] C. Xu and L. Balents, Topological Superconductivity in Twisted Multilayer Graphene, Phys. Rev. Lett. **121**, 087001 (2018).

[17] M. Ochi, M. Koshino, and K. Kuroki, Possible correlated insulating states in magic-angle twisted bilayer graphene under strongly competing interactions, Phys. Rev. B **98**, 081102(R) (2018).

[18] F. Wu, A. H. MacDonald, and I. Martin, Theory of Phonon-Mediated Superconductivity in Twisted Bilayer Graphene, Phys. Rev. Lett. **121**, 257001 (2018).

[19] Y.-H. Zhang, D. Mao, Y. Cao, P. Jarillo-Herrero, and T. Senthil, Nearly flat Chern bands in moiré superlattices, Phys. Rev. B **99**, 075127 (2019).

[20] J. Kang and O. Vafek, Symmetry, Maximally Localized Wannier States, and a Low-Energy Model for Twisted Bilayer Graphene Narrow Bands, Phys. Rev. X **8**, 031088 (2018).

[21] J. M. Pizarro, M. J. Calderón, and E. Bascones, The nature of correlations in the insulating states of twisted bilayer graphene, J. Phys. Commun. **3**, 035024 (2019).

[22] M. Koshino, N. F. Q. Yuan, T. Koretsune, M. Ochi, K. Kuroki, and L. Fu, Maximally Localized Wannier Orbitals and the Extended Hubbard Model for Twisted Bilayer Graphene, Phys. Rev. X **8**, 031087 (2018).

[23] D. M. Kennes, J. Lischner, and C. Karrasch, Strong correlations and $d + id$ superconductivity in twisted bilayer graphene, Phys. Rev. B **98**, 241407(R) (2018).

[24] H. Isobe, N. F. Q. Yuan, and L. Fu, Unconventional Superconductivity and Density Waves in Twisted Bilayer Graphene, Phys. Rev. X **8**, 041041 (2018).

[25] L. Rademaker and P. Mellado, Charge-transfer insulation in twisted bilayer graphene, Phys. Rev. B **98**, 235158 (2018).

[26] T. J. Peltonen, R. Ojajärvi, and T. T. Heikkilä, Mean-field theory for superconductivity in twisted bilayer graphene, Phys. Rev. B **98**, 220504(R) (2018).

[27] V. Kozii, H. Isobe, J. W. F. Venderbos, and L. Fu, Nematic superconductivity stabilized by density wave fluctuations: Possible application to twisted bilayer graphene, Phys. Rev. B **99**, 144507 (2019).

[28] V. Kozii, M. P. Zaletel, and N. Bultinck, Spin-triplet superconductivity from intervalley goldstone modes in magic-angle graphene, Phys. Rev. B **106**, 235157 (2022).

[29] G. Tarnopolsky, A. J. Kruchkov, and A. Vishwanath, Origin of Magic Angles in Twisted Bilayer Graphene, Phys. Rev. Lett. **122**, 106405 (2019).

[30] Z. Song, Z. Wang, W. Shi, G. Li, C. Fang, and B. A. Bernevig, All Magic Angles in Twisted Bilayer Graphene are Topological, Phys. Rev. Lett. **123**, 036401 (2019).

[31] K. Hejazi, C. Liu, H. Shapourian, X. Chen, and L. Balents, Multiple topological transitions in twisted bilayer graphene near the first magic angle, Phys. Rev. B **99**, 035111 (2019).

[32] H. C. Po, L. Zou, T. Senthil, and A. Vishwanath, Faithful tight-binding models and fragile topology of magic-angle bilayer graphene, Phys. Rev. B **99**, 195455 (2019).

[33] E. Khalaf, A. J. Kruchkov, G. Tarnopolsky, and A. Vishwanath, Magic angle hierarchy in twisted graphene multilayers, Phys. Rev. B **100**, 085109 (2019).

[34] C. Mora, N. Regnault, and B. A. Bernevig, Flatbands and Perfect Metal in Trilayer Moiré Graphene, Phys. Rev. Lett. **123**, 026402 (2019).

[35] T. Cea, N. R. Walet, and F. Guinea, Twists and the electronic structure of graphitic materials, Nano Lett. **19**, 8683 (2019).

[36] Z. Zhu, S. Carr, D. Massatt, M. Luskin, and E. Kaxiras, Twisted Trilayer Graphene: A Precisely Tunable Platform for Correlated Electrons, Phys. Rev. Lett. **125**, 116404 (2020).

[37] Y. Mao, D. Guerci, and C. Mora, Supermoiré low-energy effective theory of twisted trilayer graphene, Phys. Rev. B **107**, 125423 (2023).

[38] X. Lin, C. Li, K. Su, and J. Ni, Energetic stability and spatial inhomogeneity in the local electronic structure of relaxed twisted trilayer graphene, Phys. Rev. B **106**, 075423 (2022).

[39] Z. Ma, S. Li, M. Lu, D.-H. Xu, J.-H. Gao, and X. Xie, Doubled Moiré flat bands in double-twisted few-layer graphite, Sci. China Phys. Mech. Astron. **66**, 227211 (2023).

[40] M. Liang, M.-M. Xiao, Z. Ma, and J.-H. Gao, Moiré band structures of the double twisted few-layer graphene, Phys. Rev. B **105**, 195422 (2022).

[41] X. Zhang, K.-T. Tsai, Z. Zhu, W. Ren, Y. Luo, S. Carr, M. Luskin, E. Kaxiras, and K. Wang, Correlated Insulating States and Transport Signature of Superconductivity in Twisted Trilayer Graphene Superlattices, Phys. Rev. Lett. **127**, 166802 (2021).

[42] J. M. Park, Y. Cao, K. Watanabe, T. Taniguchi, and P. Jarillo-Herrero, Tunable strongly coupled superconductivity in

magic-angle twisted trilayer graphene, Nature (London) **590**, 249 (2021).

[43] Z. Hao, A. M. Zimmerman, P. Ledwith, E. Khalaf, D. H. Najafabadi, K. Watanabe, T. Taniguchi, A. Vishwanath, and P. Kim, Electric field-tunable superconductivity in alternating-twist magic-angle trilayer graphene, Science **371**, 1133 (2021).

[44] X. Liu, N. J. Zhang, K. Watanabe, T. Taniguchi, and J. I. A. Li, Isospin order in superconducting magic-angle twisted trilayer graphene, Nat. Phys. **18**, 522 (2022).

[45] S. Turkel, J. Swann, Z. Zhu, M. Christos, K. Watanabe, T. Taniguchi, S. Sachdev, M. S. Scheurer, E. Kaxiras, C. R. Dean, and A. N. Pasupathy, Orderly disorder in magic-angle twisted trilayer graphene, Science **376**, 193 (2022).

[46] A. Uri, S. C. de la Barrera, M. T. Randeria, D. Rodan-Legrain, T. Devakul, P. J. Crowley, N. Paul, K. Watanabe, T. Taniguchi, R. Lifshitz *et al.*, Superconductivity and strong interactions in a tunable moiré quasiperiodic crystal, Nature (London) **620**, 762 (2023).

[47] D. Călugăru, F. Xie, Z.-D. Song, B. Lian, N. Regnault, and B. A. Bernevig, Twisted symmetric trilayer graphene: Single-particle and many-body Hamiltonians and hidden nonlocal symmetries of trilayer moiré systems with and without displacement field, Phys. Rev. B **103**, 195411 (2021).

[48] F. Xie, N. Regnault, D. Călugăru, B. A. Bernevig, and B. Lian, Twisted symmetric trilayer graphene. II. Projected Hartree-Fock study, Phys. Rev. B **104**, 115167 (2021).

[49] M. Christos, S. Sachdev, and M. S. Scheurer, Correlated Insulators, Semimetals, and Superconductivity in Twisted Trilayer Graphene, Phys. Rev. X **12**, 021018 (2022).

[50] J. Y. Lee, E. Khalaf, S. Liu, X. Liu, Z. Hao, P. Kim, and A. Vishwanath, Theory of correlated insulating behaviour and spin-triplet superconductivity in twisted double bilayer graphene, Nat. Commun. **10**, 5333 (2019).

[51] P. J. Ledwith, A. Vishwanath, and E. Khalaf, Family of Ideal Chern Flatbands with Arbitrary Chern Number in Chiral Twisted Graphene Multilayers, Phys. Rev. Lett. **128**, 176404 (2022).

[52] P. J. Ledwith, E. Khalaf, Z. Zhu, S. Carr, E. Kaxiras, and A. Vishwanath, TB or not TB? Contrasting properties of twisted bilayer graphene and the alternating twist *n*-layer structures ($n = 3, 4, 5, \ldots$), arXiv:2111.11060.

[53] J. Wang and Z. Liu, Hierarchy of Ideal Flatbands in Chiral Twisted Multilayer Graphene Models, Phys. Rev. Lett. **128**, 176403 (2022).

[54] S. Zhang, B. Xie, Q. Wu, J. Liu, and O. V. Yazyev, Chiral decomposition of twisted graphene multilayers with arbitrary stacking, Nano Lett. **23**, 2921 (2023).

[55] M. Yang, Flat bands and high Chern numbers in twisted multilayer graphene, arXiv:2303.00103.

[56] X. Liu, Z. Hao, E. Khalaf, J. Y. Lee, Y. Ronen, H. Yoo, D. Haei Najafabadi, K. Watanabe, T. Taniguchi, A. Vishwanath, and P. Kim, Tunable spin-polarized correlated states in twisted double bilayer graphene, Nature (London) **583**, 221 (2020).

[57] Y. Cao, D. Rodan-Legrain, O. Rubies-Bigorda, J. M. Park, K. Watanabe, T. Taniguchi, and P. Jarillo-Herrero, Tunable correlated states and spin-polarized phases in twisted bilayer-bilayer graphene, Nature (London) **583**, 215 (2020).

[58] J. M. Park, Y. Cao, L.-Q. Xia, S. Sun, K. Watanabe, T. Taniguchi, and P. Jarillo-Herrero, Robust superconductivity in magic-angle multilayer graphene family, Nat. Mater. **21**, 877 (2022).

[59] F. K. Popov and G. Tarnopolsky, Magic angle butterfly in twisted trilayer graphene, arXiv:2305.16385.

[60] S. Carr, C. Li, Z. Zhu, E. Kaxiras, S. Sachdev, and A. Kruchkov, Ultraheavy and ultrarelativistic Dirac quasiparticles in sandwiched graphenes, Nano Lett. **20**, 3030 (2020).

[61] F. D. M. Haldane and E. H. Rezayi, Periodic Laughlin-Jastrow wave functions for the fractional quantized Hall effect, Phys. Rev. B **31**, 2529 (1985).

[62] F. K. Popov and A. Milekhin, Hidden wave function of twisted bilayer graphene: The flat band as a Landau level, Phys. Rev. B **103**, 155150 (2021).

[63] P. J. Ledwith, G. Tarnopolsky, E. Khalaf, and A. Vishwanath, Fractional Chern insulator states in twisted bilayer graphene: An analytical approach, Phys. Rev. Res. **2**, 023237 (2020).

[64] J. Wang, Y. Zheng, A. J. Millis, and J. Cano, Chiral approximation to twisted bilayer graphene: Exact intravalley inversion symmetry, nodal structure, and implications for higher magic angles, Phys. Rev. Res. **3**, 023155 (2021).

[65] J. Wang, J. Cano, A. J. Millis, Z. Liu, and B. Yang, Exact Landau Level Description of Geometry and Interaction in a Flatband, Phys. Rev. Lett. **127**, 246403 (2021).

[66] Y. Sheffer, R. Queiroz, and A. Stern, Symmetries as the guiding principle for flattening bands of Dirac fermions, Phys. Rev. X **13**, 021012 (2023).

[67] A. Parhizkar and V. Galitski, A generic topological criterion for flat bands in two dimensions, arXiv:2301.00824.

[68] G. Tarnopolsky (unpublished).